

THEORETICAL STUDIES OF THE SEISMIC RESPONSE OF COLUMN-SUPPORTED
COOLING TOWERS

C. S. Gran^I, T. Y. Yang^{II} and J. L. Bogdanoff^{III}

SUMMARY

A column-supported TVA cooling tower is modeled using orthotropic plate and beam finite elements. Its time-history response to 30 seconds of the N-S acceleration component of the 1940 El Centro earthquake is computed by the modal superposition technique. Spectral analysis estimates the tower's maximum response with 4% critical damping. Shell internal loads indicate membrane behavior dominates. A new doubly-curved membrane shell finite element is developed to facilitate future analysis. The in-plane displacement assumptions are complete bicubics, transverse is bilinear. Condensed to 28 D.O.F., the element contains three implicit rigid body modes which are sufficient to produce excellent convergence characteristics with improved efficiency.

INTRODUCTION

Several studies of the seismic response of large, column-supported cooling towers have established the necessity of including the supporting columns in the analytical model (1,2). The authors' initial investigation of cooling tower behavior employed a finite element idealization in which the columns were represented by beam finite elements and the hyperbolic shell was modeled by orthotropic, quadrilateral plate elements (3). This modeling technique was found to yield excellent results for natural frequencies and mode shapes and equally good results for the time history response of deflections when the tower was subjected to a given earthquake record. However, the element mesh was necessarily coarse in order to study general trends and establish the validity of the method. Presented herein are the results obtained by making a substantial mesh refinement.

Membrane forces are found to dominate the shell's response. This phenomenon suggests the use of a finite element modeling that will accurately represent the state of stress with the greatest efficiency. That is, in the shell boundary region where bending is considerable, a high-order general bending element is used, while away from the edge, where membrane action prevails, a sophisticated membrane element is employed. This procedure would result in a large reduction in the number of equations required to solve the problem with a high degree of accuracy. As the first step towards the realization of this solution process, the formulation and testing of a new high-order, doubly-curved membrane shell finite element, specialized for application to cooling tower shells, is presented.

SEISMIC RESPONSE OF THE PARADISE COOLING TOWER

A cooling tower in Unit 3 of the 1200 MW TVA fossil fuel power plant at Paradise, Kentucky, USA (Fig. 1) is studied. This cooling tower is in seismic risk zone 1. A detailed description of the reinforced concrete tower and the finite elements used to model the system is given in Ref. 3.

-
- I Structural Engineer, The Aerospace Corporation, Los Angeles, California, USA
II Professor and Head, School of Aeronautics and Astronautics, Purdue University, West Lafayette, Indiana, USA
III Professor, School of Aeronautics and Astronautics, Purdue University, West Lafayette, Indiana, USA

Eccentric Modes. Only those modes with one circumferential wave are responsive to horizontal earthquake excitation (2, 3). These eccentric modes can be accurately predicted using a finite element model of half of the actual shell surface (4). Several different half-shell mesh configurations are used to model the Paradise cooling tower. These element mesh sizes, given as number of meridional shell elements X number of circumferential elements, include: 4 x 10 (345 DOF), 8 x 10 (573 DOF), 9 x 10 (654 DOF), and 9 x 10 (918 DOF). The 918 DOF model differs from the others in that it uses two beam finite elements to represent each column except for the column at one edge ($\theta = 0^\circ$). This particular column is formed by six beam elements in order to find detailed stress information along the column length. All the above models feature beam elements to form the top ring-beam of the shell, orthotropic quadrilateral plate elements with a triangular variation at the base to form the shell, and beam elements to form the discrete column supports. The 9 x 10 model is shown in Fig. 2.

The first three eccentric frequencies of these models are presented in Table 1. Slight aberrations within the convergence pattern are likely to be caused by the extreme sensitivity of frequencies to changes in meridional curvature. The corresponding meridional shapes of the 918 DOF model are reasonable. The circumferential shape of all three modes remains circular throughout the body of the shell. However, the triangular elements affect this shape at the shell base. Inequities in the distribution of lumped mass resulting from elements of different size meeting at alternating nodal points produce a number of waves equal to one-half the number of column pairs. The deviation from a circular shape is slight in the first eccentric mode, practically non-existent in the second mode and pronounced in the third. The third eccentric mode is not of primary concern simply because the earthquake response of the cooling tower is dominated by the first mode with a slight contribution from the second mode.

Earthquake Response. The 9 x 10 model with 918 DOF is used to determine the time-history of deflections when 30 seconds of the North-South acceleration component of the 18 May 1940 El Centro earthquake is applied parallel to the plane of symmetry. The first three eccentric modes are included in the modal superposition analysis, each with zero damping. The radial deflection along a meridian at $\theta = 0^\circ$, where θ is measured from the plane of symmetry, is shown in Fig. 3 for two critical instances of maximum shell tip deflection (8.43 in. at 11.48 sec.) and maximum column top deflection (3.78 in. at 10.56 sec.). The circumferential shapes remain circular with a slight wavy distribution at the shell base.

The maximum individual modal responses of the first three eccentric modes are computed by the response spectrum method. The longitudinal distribution of radial deflection at $\theta = 0^\circ$ is presented in Fig. 4 for the case in which 4% critical damping has been assumed for each mode. Figure 4 illustrates the rapidly diminishing effect of the higher modes upon the total response. In the undamped case, the first mode contributes approximately 90% of the total, while the second and third modes contribute 9% and 1%, respectively. When 4% damping is included, the first mode accounts for over 96% of the total response, the second mode adds approximately 4%, and the third mode's contribution is negligible. Also, the inclusion of 4% viscous damping decreases the maximum deflections by approximately 60%.

Internal Loads. The three modal responses with 4% damping are combined by the root-mean-square (RMS) technique to determine the total maximum response of the cooling tower. This state of deflection is enforced in the determination of the maximum forces and stresses produced in the structure. The contribution of gravity is included.

The longitudinal distributions of meridional and circumferential bending moment in the shell at $\theta = 0^\circ$ are shown in Figs. 5 and 6, respectively. Approximately 35 ft. above the base of the shell, the moments become nearly zero which indicates predominantly membrane behavior. The longitudinal distributions of meridional membrane force at $\theta = 180^\circ$ and circumferential membrane force at $\theta = 0^\circ$ are shown in Figs. 7 and 8, respectively. Under the present conditions, stresses are extremely low and the shell would persevere with no damage.

Axial forces in the columns play a crucial role in determining the cooling tower's response (2, 5). In this study, the compressive force in the most critical column is less than the crushing load of the column material and well below the critical buckling load. However, the maximum tensile forces slightly exceed the reinforcement yield strength. It appears that some columns will undergo inelastic deformations. Such behavior will increase both the flexibility and the damping of the structure to a degree dependent upon the column's ductility. These alterations can be accounted for in a linear elastic analysis such as this, by a reduction of the design load as suggested in Ref. 6.

It should be noted that the modeling of each column by only one beam element is inadequate as it yields bending moments at the column top which are larger than those at the base. At least two beam elements per column are necessary to produce a satisfactory moment distribution. Decreasing element length increases beam stiffness terms and smoothens the large variation in stiffness quantities at the shell-column joints.

A HIGH-ORDER, DOUBLY-CURVED MEMBRANE SHELL FINITE ELEMENT

In the preceding analysis, the cooling tower shell behaves primarily as a membrane. The only appreciable bending is confined to a narrow band at the shell base which is less than 9% of the overall shell height. A more efficient solution to this problem could be obtained by using the procedure outlined in the introduction. The formulation of a membrane shell finite element required to pursue such a method is presented.

Element Derivation. The present doubly-curved shell element is a quadrilateral defined by lines of principal curvature, specialized for application to shells of revolution. An array of eight mapping nodes specifies a cubic variation of R and Z in the meridional direction (Fig. 9) allowing initial element geometry to exactly model meridional shapes that are third order or less. The interpolation functions for R and Z are detailed in Ref. 7. The in-plane displacement assumptions are complete bicubics, composed of products of one-dimensional first-order Hermitian interpolation polynomials. The transverse displacement assumption is complete bilinear. Composed of products of one-dimensional, zeroth-order Hermite polynomials. Element shape functions are given explicitly in Ref. 7. The element stiffness and mass matrices are derived by well known energy methods. Integration is accomplished by applying the 5 x 5 Gauss quadrature formula. Initially, the element has 36 DOF. However, mixed partial derivative DOF are eliminated from the displacement vector following the Guyan reduction process. In its final form, the element possesses 28 DOF.

Rigid Body Modes. Finite element displacement functions must include rigid body modes to insure convergence with mesh refinement. A good representation of rigid body modes will enhance the convergence rate allowing better results to be

obtained with fewer equations. The eigenvalues of the present element stiffness matrix show that three rigid body modes corresponding to the two inplane translations and a rotation about the normal to the shell are implicitly included in the element formulation. As expected, the accuracy of their representation increases with element refinement.

Cooling Tower under Dead Load. The fixed-base cooling tower shown in Figure 10, subjected to its own dead load, has been analyzed by Fonder and Clough (8) using a doubly curved quadrilateral element with 24 DOF. Results for membrane forces are presented in Fig. 11. Fonder and Clough used 20 elements with a total of 122 DOF, although fewer elements might have been needed to obtain similar results. These elements do not contain rigid body motion terms. With rigid body modes explicitly added to their elements, Fonder and Clough found that the results are far from the exact solution.

When the present element is used to model this cooling tower, several different mesh configurations are employed. Due to the problem's axisymmetric nature, the circumferential displacement and all circumferential derivatives are suppressed. In each case, the mesh is one element wide, spanning a 5° angle. The two-element mesh involves 14 DOF, four elements require 26 DOF, six elements use 38 DOF, and the eight-element mesh contains 50 DOF. The circumferential and meridional membrane forces thus calculated are shown in Fig. 11. Results for each mesh size compare quite well with those of Ref. 8. The slight discrepancy in the meridional membrane force at the base of the shell is due to the fact that bending moments become appreciable in this region and the present element will not account for such behavior. The excellent results of coarse mesh sizes and the rapid convergence exhibited can be attributed to the accurate representation of the necessary rigid body modes contained in the present element formulation.

First Eccentric Mode Frequency of Cooling Tower. The natural vibration of a fixed-base cooling tower shown in Fig. 12 is now investigated. The modulus of elasticity is 3×10^6 psi, Poisson's ratio is 0.15, and the mass density of 0.225×10^{-3} lb-sec²/in⁴. Of particular interest is the first vibration mode with one circumferential wave which has been shown to have a dominant role in the seismic response of cooling towers. Several authors have performed an eigenvalue analysis of this tower (3, 9, 10, 11). Their results for the frequency of the first eccentric mode are given in Table 2.

In the present example, however, only the membrane strain energy is considered. It has been shown that the membrane energy dominates the total strain energy for vibration modes with a low circumferential wave number (10). Thus it is expected that neglecting the bending contribution will cause only a slight reduction in frequency from the general case. The two purely membrane solutions presented in Table 2 agree well not only with each other but also with the other general solutions.

One of the membrane solutions is obtained using the 12 DOF quadrilateral membrane plate element of the NASTRAN program. Four different mesh configurations are employed, each of which models one-half of the shell surface. Such a model is the minimum size necessary to accurately prescribe the boundary conditions. Figure 13 shows the NASTRAN solution apparently converging to the present membrane shell element solution.

Fig. 13 also shows the frequency solutions obtained using several mesh sizes of the present element. In this example, each of the present element's degrees-of-freedom participates to some extent, fully exploiting the element's potential. The solution rapidly converges requiring an order of magnitude fewer equations than the NASTRAN approach. The present element, with its ability to accurately capture the shell geometry along with its high-order displacement functions, is considerably more efficient than the multifaceted flat plate approximation.

CONCLUSIONS

The realistic modeling of column-supported cooling towers using quadrilateral plate and beam finite elements has been found to accurately predict natural frequencies and mode shapes. One beam element per column is sufficient for this purpose, however, two or more may be required to obtain detailed internal loads.

Only those modes with one circumferential wave are excitable by horizontal earthquake motion. In this study, the contributions of the higher eccentric modes to the total deflection rapidly diminish. In the undamped case, the first mode contributes approximately 90% of the total deflection. Its participation is 96% when 4% critical damping is included.

Consideration must be given to the discrete supporting columns as they are found to be the vulnerable region. Column axial forces in particular appear to be most critical. The shell response is characterized by membrane behavior. In the case studied, bending was restricted to a region at the shell base of less than 9% of the overall shell height.

The 9 x 10 element mesh with 918 DOF is practically sufficient for the purpose of predicting the cooling tower's dynamic behavior. Triangular elements at the shell base produce a slight wave form, however, their use is justified by the considerable savings in computational time while detrimental effects are minimal. For more detailed predictions, sophisticated high-order shell finite elements could be used.

A high-order doubly-curved membrane shell finite element is developed for application to cooling tower studies. Third-order meridional mapping contributes to excellent results for geometry-sensitive frequencies. Bicubic in-plane displacement functions implicitly include three rigid body modes, two in-plane translations and rotation about the normal. These modes are sufficient to produce excellent convergence for curved membrane shells. Once this element has been merged with beam and general bending shell elements, it is believed that accurate and efficient solutions to the cooling tower problem can be obtained.

ACKNOWLEDGMENTS

The authors gratefully acknowledge the support of the National Science Foundation through grant GI41897. Valuable suggestions from J. L. Bogdanoff are also acknowledged.

REFERENCES

1. A. K. Gupta and W. C. Schnobrich, "Seismic analysis and design of hyperbolic cooling towers". Nuclear Engng Design, Vol.36, 1976, pp. 251-260.

2. Gould, P. L., Sen, S. K., and Suryoutomo, "Seismic analysis of hyperbolic cooling towers by the response spectrum method," Inter. Symp. Earthquake Structural Mech., St. Louis, Missouri, August 1976.
3. Gran, C. S., and Yang, T. Y., "NASTRAN and SAP IV Applications on the Seismic Response of Column-Supported Cooling Towers," J. Comput Structure, Vol. 8, No. 6, June, 1978, pp. 761-768.
4. Gran, C. S. and Yang, T. Y., "Refined Analysis of the Seismic Response of Column-Supported Cooling Tower," to appear in J. Comput Structure.
5. W. C. Schnobrich and A. K. Gupta, "Design of Cooling Towers to Resist Earthquakes," Dept. of Civil Engineering, Univ. of Illinois, Urbana.
6. Newmark, N. M. and Rosenblueth, E., Fundamentals of Earthquake Engineering, Prentice Hall, Englewood Cliffs, 1971.
7. Gran, C. S. and Yang, T. Y., "Doubly Curved Membrane Shell Finite Element," J. Engng. Mech. Div., ASCE, Vol. 105, August 1979, pp. 567-584.
8. Fonder, G. A. and Clough, R. W., "Explicit Addition of Rigid-Body Motions in Curved Finite Elements," AIAA Journal, Vol. 11, March 1973, pp. 305-312.
9. Carter, R. L., Robinson, A. R., and Schnobrich, W. C., "Free Vibration of Hyperboloidal Shells of Revolution," J. Engng. Mech. Div., ASCE, Vol. 95, October 1969, pp. 1033-1052.
10. Hashish, M. G., and Abu-Sitta, S. H., "Free Vibration of Hyperbolic Cooling Towers," J. Engng. Mech. Div., ASCE, Vol. 97, April 1971, pp. 253-269.
11. Sen, S. K., and Gould, P. L., "Free Vibration of Shells of Revolution Using FEM," J. Engng Mech. Div., ASCE, Vol. 100, April 1974, pp. 283-303.

Table 1. Natural frequencies (Hz.) of modes with one circumferential wave for the Paradise cooling tower

Longitudinal Mode	Element Mesh (DOF)			
	4 x 10 (345)	8 x 10 (573)	9 x 10 (654)	9 x 10 (918)
1.	2.1952	2.1924	2.1962	2.1850
2	3.8723	3.6612	3.6438	3.6377
3	7.8041	7.6335	7.7131	7.6755

Table 2. General and membrane solutions for first eccentric frequency of fixed-base cooling tower

Solution technique	Frequency (Hz)	CDC 6500 CP time (min.)
Present membrane shell	3.2708	1.0
finite element (37 and 51 DOF)	3.2696	1.7
NASTRAN membrane plate elements (319 DOF)	3.2768	6.4
Numerical integration (9)	3.2884	
Finite difference (10)	3.3345	
Curved shell of revolution elements (11)	3.2910	
SAP IV plate elements (3) (384 DOF)	3.3119	29.0

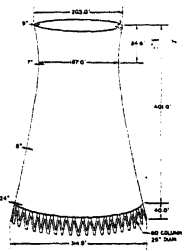


Fig. 1. The Paradise cooling tower.



Fig. 2. The finite element modeling of the Paradise cooling tower.



Fig. 3. The radial deflection of the meridional line at $\theta = 0^\circ$ at the time of maximum shell tip deflection ($t=11.48$ sec) and maximum column top deflection ($t = 10.56$ sec).

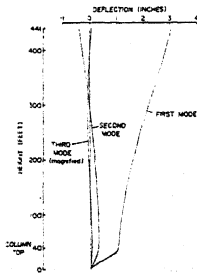


Fig. 4. Maximum individual radial deflections of the first three eccentric modes with 4% damping (with the third mode magnified ten times).

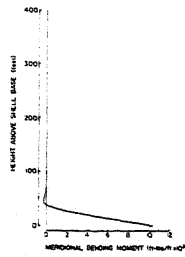


Fig. 5. Longitudinal distribution of meridional bending moment at $\theta = 0^\circ$.

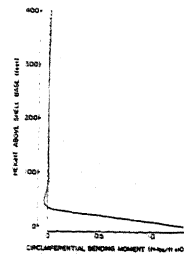


Fig. 6. Longitudinal distribution of circumferential bending moment at $\theta = 0^\circ$.

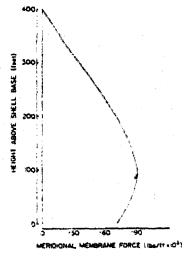


Fig. 7. Longitudinal distribution of meridional membrane force at $\theta = 180^\circ$.

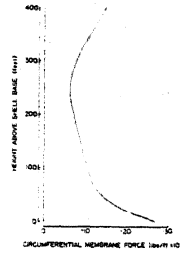


Fig. 8. Longitudinal distribution of circumferential membrane force at $\theta = 0^\circ$.

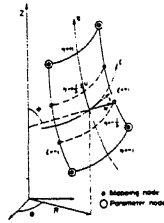


Fig. 9. High-order doubly curved membrane shell finite element.

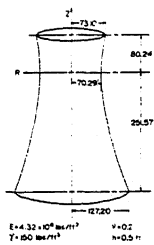


Fig. 10. Cooling tower under dead load.

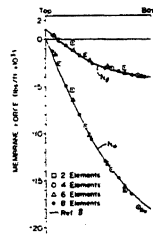


Fig. 11. Membrane forces in cooling tower under dead load.

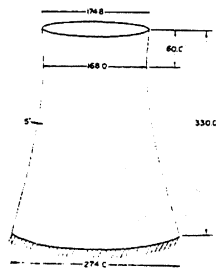


Fig. 12. Cooling tower used for free vibration analysis.

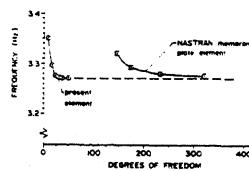


Fig. 13. First eccentric frequency of hyperbolic cooling tower.